

Early Indosinian Weiya Gabbro in Eastern Tianshan, China: Elemental and Sr-Nd-O Isotopic Geochemistry, and Its Tectonic Implications

ZHANG Zunzhong^{1,2}, GU Lianxing^{1,*}, WU Changzhi¹,
ZHAI Jianping², LI Weiqiang¹ and TANG Junhua¹

*1 State Key Laboratory of Mineral Deposit Research (Nanjing University),
Department of Earth Sciences, Nanjing University, Nanjing, Jiangsu 210093*

2 School of the Environment, Nanjing University, Nanjing, Jiangsu 210093

Abstract: The Weiya gabbro in eastern Tianshan was formed during the early Indosinian. This rock, with low ratios of Ce/Pb (5.74–10.16), is notably characterized by enrichment in large ion lithophile elements (LILE), such as Rb, K, Ba and Pb, and in high field strength elements (HSFE), such as U and Th, but depletion in Nb and Ta. All samples of the Weiya gabbro display similar chondrite-normalized patterns with moderate enrichment in LREE (72.58–135.61ppm), moderate depletion in HREE (15.26–25.31ppm) and mild fractionation between LREE and HREE (L/H=4.09–5.98). The average initial Sr value of the rock is 0.7069, and $\delta^{18}\text{O}$ values of the rock range from 5.67‰–8.04‰. In terms of Nd isotope ratios, the Weiya gabbro is characterized by positive $\varepsilon_{\text{Nd}}(t)$ values (0.52–0.76). All these characteristics indicate that the source region of the Weiya gabbro was metasomatized by fluids released from subducted young continental crust, with limited crustal contamination during magma ascent and emplacement. Continental (A-type) subduction was induced by northward subduction of the Paleo-Tethyan oceanic plate during the latest Permian to Triassic. From this point of view, it is supposed that tectonic conversion from the Paleo-Asian to the Paleo-Tethys regime occurred during the latest Permian or earliest Triassic.

Key words: Weiya gabbro, mantle metasomatism, intra-continental subduction, eastern Tianshan, Xinjiang

1 Introduction

Based on research on tectonothermal events in the eastern Tianshan Mountains, previous contributions (Hu et al., 1997; Li et al., 2003) suggested that major events of continental collision between the Siberian Craton to the north and the Tarim Craton to the south occurred around 300 Ma in this area. Then, tectonics converted from compression to extension, resulting in extension of the eastern Tianshan area and subsequent emplacement of numerous mafic and ultramafic rocks and coeval granitoids (Gu et al., 1996, 1999; Han et al., 1997, 1999; Hong et al., 2004; Zhou et al., 2004). Some authors (Gu et al., 2003; Li et al., 2005; Zhang et al., 2005) have addressed the manifestation of Indosinian (Triassic) magmatism and mineralization in the eastern Tianshan Mountains, but their relationship to regional tectonics remains to be evaluated. As a consequence, it remains to be understood whether the

Indosinian tectonism was a continuation of the Hercynian post-collisional extension in eastern Tianshan or was affected substantially by other tectonic system. Although it has been emphasized (Han et al., 1997; Jahn et al., 2000; Zhao et al., 2004; Zhou et al., 2004; Li et al., 2005; Xia et al., 2005; Zhang et al., 2005) that mantle-derived magmas played a direct or indirect role in the formation of granitoids and mineralization in the eastern Tianshan Mountains and Central Asian Orogenic Belt, little is known about the nature, origin and tectonic setting of these magmas.

This paper focuses on earliest-formed Weiya gabbro within the Weiya complex with ages ranging between 246–233Ma (Zhang et al., 2005) in the eastern Tianshan Mountains in order to provide geochemical and Sr-Nd-O isotope data to (1) document its possible source(s), (2) constrain its petrogenesis, and (3) further discuss its tectonic implications.

* Corresponding author. E-mail: lxgu@nju.edu.cn.

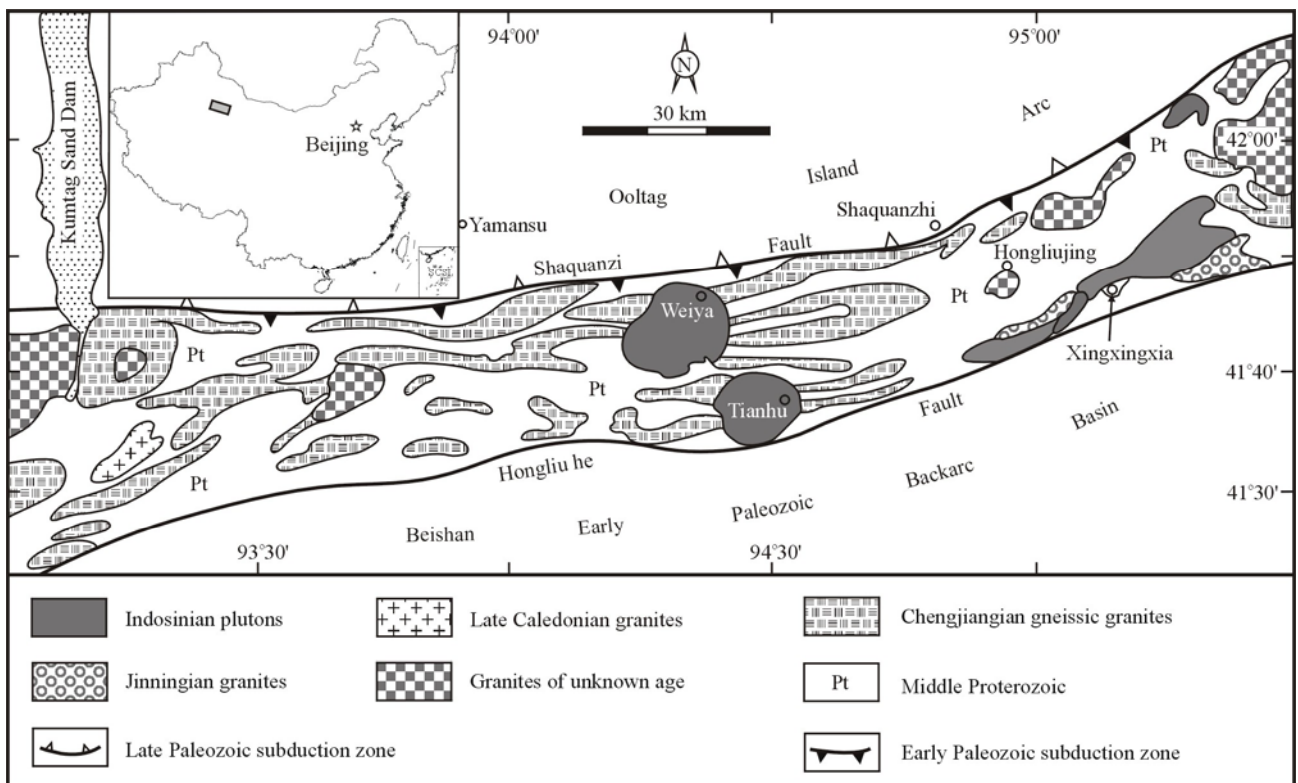


Fig. 1. Regional geology of the eastern section of the Middle Tianshan belt.

2 Geological Setting and Geology of the Weiya Complex

An elongated metamorphic belt in the eastern section of the Tianshan orogenic belt is bounded by the Shaquanzi fault to the north and the Hongliuhe fault to the south, and is referred to as the Middle Tianshan Mountains (Fig. 1). Precambrian volcano-sedimentary strata that are composed mainly of schists, gneisses, marbles, amphibolites and migmatites have been divided into the Mesoproterozoic Xingxingxia Group and Kawabulake Group, which were deformed and metamorphosed around 1000 Ma, and the Neoproterozoic Tianhu Group, which was deformed and metamorphosed around 700 Ma (Hu et al., 1997).

The Middle Tianshan Mountains can be geologically correlated to a zone on the northern margin of the Tarim Precambrian continent far to the south. Thus, this metamorphic belt is interpreted to have been pulled apart from the Tarim continent by the early Paleozoic back-arc extension induced by the southward subduction of the Tianshan Ocean along the Shaquanzi fault (Fig. 1), and is considered as an internal block within the Paleozoic Tianshan orogen (Hu et al., 1990; Guo and Zhang, 1993). The subduction of the Tianshan Ocean was converted in direction towards the north at the beginning of the late Paleozoic (Fig. 1), resulting in the Qoltag island arc belt on the southern margin of the Kazakhstan Plate (Gu et al., 1990;

Wu et al., 2006). The Qoltag island arc and the Middle Tianshan passive continental margin collided along the Shaquanzi fault as the subducting Tianshan Ocean was completely consumed in the late Carboniferous (Gu et al., 2001; Li et al., 2003), resulting in a dextral ductile-shear zone along the Shaquanzi fault (Shu et al., 1999).

The Weiya complex is situated near the Weiya station of the Lanzhou-Xinjiang railway and is 130 km to the southeast of the city of Hami, Xinjiang Uygur Autonomous Region. Tectonically, it belongs to the eastern section of the Middle Tianshan Precambrian belt (Fig. 1). The Weiya complex (Fig. 2), with nearly elliptical outline and an outcrop area of approximately 200 km², intruded Meso- to Neoproterozoic schists and gneisses and is free of deformation or metamorphism. Based on field observations, six intrusive phases have been recognized in a sequence of gabbro, quartz syenite, quartz diorite, biotite monzogranite, quartz diorite porphyrite (dykes) and fine-grained granite.

The gabbroic rock is situated in the northeastern part of the Weiya complex and forms five small intrusions with an outcrop area of about 1 km² in total (Fig. 2). This is a dark green and medium- to fine-grained massive rock. It is composed mainly of clinopyroxene (35%–40%), plagioclase (An₅₅₋₆₅, 40%–45%) and hornblende (5%–15%), with minor amounts of primary carbonate (0–5%). No olivine or orthopyroxene has been discerned. Accessory minerals are dominated by apatite, Ti-Fe oxides and zircon.

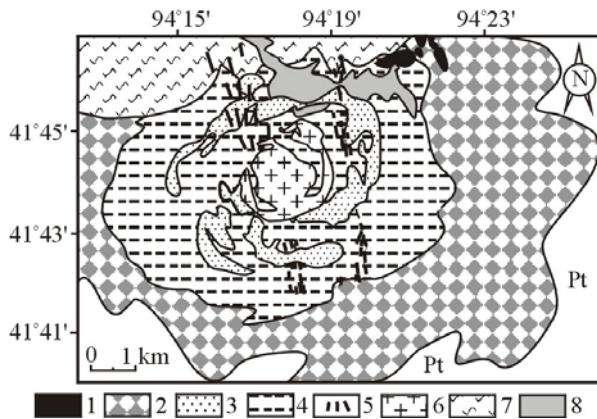


Fig. 2. Geological map of the Weiya complex.

1. gabbro; 2. quartz syenite; 3. quartz diorite; 4. monzogranite; 5. dykes of quartz diorite porphyrite; 6. fine-grained granite; 7. Mesoproterozoic gneisses; 8. Quaternary sediments; Pt - Proterozoic.

3 Analytical Methods

Hand specimens (approximately 1–2 kg) were collected and crushed by a crocodile-type grinder into slabs less than 0.5 mm in size. A quarter of each sample was obtained by the “cone and quarter method”. This split was ground by a ball-grinder to pass 200 mesh. A 50-g fraction of the powder was further ground and homogenized by hand in an agate mortar and pestle under alcohol, and then dried for chemical and Sr-Nd-O isotopic analyses.

Major oxides such as Fe_2O_3 and FeO are analyzed by the wet chemistry method at the Analysis Center of the Department of Earth Sciences, Nanjing University with analytical uncertainties better than 0.5%–1%. Other major elements were measured on a VF320 single-channel X-ray fluorescence spectrometer (XRF) at the Modern Analysis Center, Nanjing University with analytical uncertainties better than $\pm 5\%$. Trace elements (including rare earth elements) were analyzed at the State Key Laboratory of Mineral Deposit Research (Nanjing University) on an Element-2 high-resolution inductively coupled plasma mass spectrometer (ICP-MS) after the method described by Gao et al. (2003). The precision is generally better than 5% for most trace elements with concentrations greater than 10 ppm, and 10% for those less than 10 ppm.

Oxygen isotope analyses were performed on a MAT-252 mass spectrometer at the State Key Laboratory for Mineral Deposit Research (Nanjing University). The results are reported in the standard δ notation as per mill (‰) deviation from the Vienna SMOW standard. Precisions are better than 0.2 per mill. Rb, Sr, Sm and Nd abundances were also obtained by isotope dilution. Dissolution and chemical separation of Sm-Nd and Rb-Sr samples were accomplished using a procedure similar to that described in Wang et al. (1988). All Sr data are corrected for mass fractionation to $^{86}\text{Sr}/^{88}\text{Sr} = 0.1194$ and reported relative to

a value of $^{87}\text{Sr}/^{86}\text{Sr} = 0.710239 \pm 8$ ($2s$) for NBS-987 standard. In the Nd isotopic analysis, $^{146}\text{Nd}/^{144}\text{Nd} = 0.7219$ was taken as the standard for mass-fractionation correction, and Nd isotopic ratios were normalized to a value of $^{143}\text{Nd}/^{144}\text{Nd} = 0.511864 \pm 6$ ($2s$) for La Jolla. Overall blanks are about less than 3×10^{-9} g for Rb and Sr, and 9×10^{-11} g for Sm and Nd, respectively. The decay constants used in calculation are $^{87}\text{Rb} = 0.0142 \text{ Ga}^{-1}$, and $^{147}\text{Sm} = 0.00654 \text{ Ga}^{-1}$.

The notation of $\varepsilon_{\text{Nd}}(t)$ is defined (Hu et al., 2000) as

$$\varepsilon_{\text{Nd}}(t) = \varepsilon_{\text{Nd}}(0) - Q \times f \times t$$

where, $\varepsilon_{\text{Nd}}(0) = [({}^{143}\text{Nd}/{}^{144}\text{Nd})_{\text{S}} / ({}^{143}\text{Nd}/{}^{144}\text{Nd})_{\text{CHUR}} - 1] \times 10000$, S = Sample and $({}^{143}\text{Nd}/{}^{144}\text{Nd})_{\text{CHUR}} = 0.512638$, $Q = 25.1 \text{ Ga}^{-1}$, $f = f_{\text{Sm}/\text{Nd}} = [({}^{147}\text{Sm}/{}^{144}\text{Nd})_{\text{S}} / ({}^{147}\text{Sm}/{}^{144}\text{Nd})_{\text{CHUR}}] - 1$, $({}^{147}\text{Sm}/{}^{144}\text{Nd})_{\text{CHUR}} = 0.1967$, and $t = 0.24 \text{ Ga}$.

4 Geochemistry

4.1 Major elements

As shown in Table 1, the contents of SiO_2 , MgO and CaO of this rock range between 43.51–49.04 wt%, 5.09–9.27 wt% and 8.72–20.64 wt%, respectively. All samples are plotted along the calc-alkaline field in the total alkaline vs. silica (TAS) diagram (not shown). $\text{Mg}^\#$ values [$100 \times \text{Mg}/(\text{Mg} + \text{Fe}^{2+})$, molar ratio] of the rock range between 35.34–57.56 (Table 1) and are lower than that of undifferentiated primitive magma (60–71, Langmuir et al., 1977), indicating that the Weiya gabbro was not crystallized directly from a primitive magma, but was formed by a magma that had experienced fractional crystallization of olivine and clinopyroxene (Fig. 3). Furthermore, as can be seen in Fig. 3, Al_2O_3 content increases with decreasing CaO and MgO , suggesting that plagioclase was not involved in fractional crystallization.

Some samples (such as sample x-39 and x-45) show lower CaO , MgO and TiO_2 contents but higher Al_2O_3 , Na_2O , K_2O and P_2O_5 contents than others (Table 1), indicating that these samples might have lower modal abundance of clinopyroxene and higher modal abundance of plagioclase, apatite and primary carbonate.

4.2 Trace and rare earth elements

The Weiya gabbro is notably characterized by enrichment in large ion lithophile elements (LILE) (such as Rb, K, Ba and Pb, of which Ba is the most enriched), and enrichment in high field strength elements (HSFE) such as U and Th, but depletion in HFSE such as Nb and Ta (Table 1; Fig. 4). Such geochemical features of mafic rocks are commonly interpreted either as being subduction-related or related to intense crustal contamination (Li et al., 1998a; Jahn et al., 2004). Negative anomalies of P (and Sr) in some samples (Fig. 4) are likely related to fractional crystallization of apatite

Table 1 Major oxides (wt%) and trace element abundances (ppm) of the Weiya gabbro

Sample	x-39	x-45	x-47	x-48	x-50	x-51
SiO ₂	48.46	49.04	46.91	47.33	45.41	43.51
TiO ₂	1.43	1.50	2.29	2.59	2.83	3.44
Al ₂ O ₃	18.02	13.79	9.85	12.44	11.39	14.63
Fe ₂ O ₃	2.16	2.38	1.94	3.52	2.59	2.53
FeO	7.37	5.44	5.09	5.69	5.50	4.32
MnO	0.11	0.16	0.12	0.14	0.11	0.08
MgO	5.09	6.45	9.27	7.09	8.20	7.30
CaO	8.72	14.76	20.64	16.77	18.46	18.23
Na ₂ O	3.95	2.59	0.77	1.80	1.32	0.94
K ₂ O	1.37	1.07	0.39	0.74	0.69	1.10
P ₂ O ₅	0.74	0.98	0.20	0.23	0.24	0.13
LOI	2.38	1.53	2.41	1.50	3.14	3.93
Total	99.80	99.69	99.88	99.84	99.88	100.14
Sc	16.80	33.59	26.11	34.29	24.33	18.80
Ti	8352.00	8669.00	13265.00	13813.00	15860.00	19882.00
V	162.87	249.10	131.56	225.11	216.33	186.90
Co	33.74	20.13	15.32	20.69	15.30	13.11
Ga	17.81	15.09	14.57	17.69	15.81	17.78
Rb	43.46	37.45	8.78	16.77	12.33	39.73
Sr	593.20	714.90	221.20	389.00	179.80	242.50
Y	23.63	36.04	21.56	33.19	25.45	35.81
Zr	55.10	81.30	251.30	208.60	223.10	293.40
Nb	1.55	3.13	4.36	3.15	2.05	2.46
Ba	1570.00	1021.00	246.00	1148.00	603.00	847.00
Hf	1.31	1.90	6.98	6.35	5.86	6.21
Ta	0.16	0.28	0.43	0.21	0.26	0.35
Pb	6.62	5.78	3.23	4.66	4.84	6.05
Th	1.78	3.19	2.79	2.52	1.47	2.29
U	0.78	2.56	1.30	1.07	0.44	0.60
La	18.36	24.46	13.94	17.96	11.13	14.78
Ce	40.95	56.41	32.82	44.05	27.79	37.76
Pr	5.70	7.88	4.63	6.32	4.35	5.88
Nd	24.54	35.10	20.41	29.45	21.15	27.39
Sm	5.30	7.74	4.65	7.72	5.08	6.79
Eu	3.06	4.01	2.08	3.28	3.09	4.12
Gd	5.64	8.49	4.61	7.10	5.56	7.38
Tb	0.69	1.05	0.62	0.91	0.72	0.98
Dy	4.45	6.79	3.94	6.24	4.81	6.47
Ho	0.89	1.39	0.83	1.25	0.97	1.31
Er	2.39	3.85	2.37	3.58	2.62	3.74
Tm	0.29	0.46	0.33	0.49	0.36	0.47
Yb	1.80	2.88	2.21	3.15	2.22	2.88
Lu	0.24	0.40	0.35	0.51	0.37	0.44
Mg [#]	35.34	45.97	57.56	44.46	51.15	52.53
Th/Yb	0.99	1.11	1.26	0.80	0.66	0.79
Ta/Yb	0.09	0.10	0.20	0.07	0.12	0.12
Ti/Zr	151.58	106.63	52.79	66.22	71.09	67.76
Ti/Y	353.46	240.56	615.23	416.20	623.25	555.20
Ce/Pb	6.19	9.77	10.16	9.46	5.74	6.25
Ba/Nb	1012.90	326.41	56.42	364.10	293.86	344.73
La/Nb	11.84	7.82	3.20	5.70	5.42	6.02
LREE	97.90	135.61	78.53	108.78	72.58	96.72
HREE	16.37	25.31	15.26	23.22	17.63	23.67
L/H	5.98	5.36	5.15	4.68	4.12	4.09
δEu	1.70	1.51	1.36	1.33	1.77	1.77

instead of crustal contamination. This is because that apatite is both the main P-bearing mineral within the upper mantle (Smith, 1981) and significant carrier (Frey et al., 1980) of light rare earth elements (LREE). As a consequence, fractional crystallization of this mineral could account for depletion in P (and Sr) and LREE. This

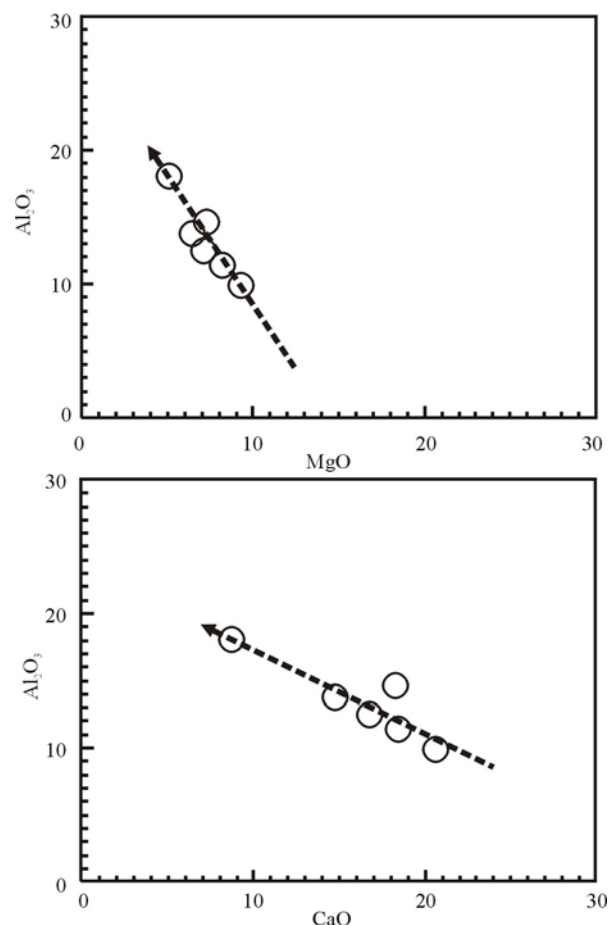


Fig. 3. Variation plots of Al₂O₃ (wt%) vs. MgO (wt%) and Al₂O₃ (wt%) vs. CaO (wt%) for the Weiya gabbro.

is well consistent with our analyses listed in Table 1.

All samples of the Weiya gabbro display similar chondrite-normalized patterns (Fig. 5) with moderate enrichment in LREE (72.58–135.61ppm), moderate depletion in HREE (15.26–25.31ppm) and mild fractionation between LREE and HREE (L/H=4.09–5.98, Table 1). Moreover, the rock shows distinctively positive Eu anomalies (Fig. 5), suggesting that insignificant amount of or even no plagioclase was retained in the residue during partial melting, or that plagioclase was not involved in fractional crystallization at lower pressures. This is in good agreement with the above-mentioned major element geochemical data.

4.3 Sr-Nd-O isotopic compositions

As shown in Table 2, the Weiya gabbro has initial Sr values ranging from 0.7066 to 0.7077 with an average of 0.7069, and initial Nd values ranging from 0.512356 to 0.512368 with an average of 0.512365, respectively. Positive $\epsilon_{Nd}(t)$ values (0.52–0.76, Table 2) imply that this rock is derived from mildly depleted mantle. In the range of 5.67‰–8.04‰, some of the $\delta^{18}O$ values (Table 2), such as that of sample x-51, fall out of the range of mantle-derived primitive magmas (e.g. 5.0‰–7.0‰, Kyser, 1990),

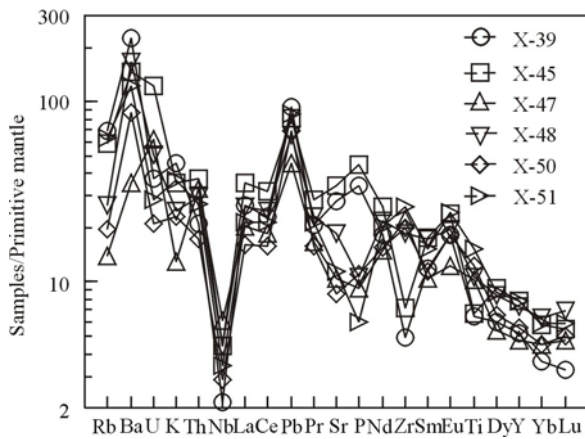


Fig. 4. Primitive mantle-normalized spider diagram of trace elements for the Weiya gabbro. Normalized values of primitive mantle are from Sun and McDonough (1989).

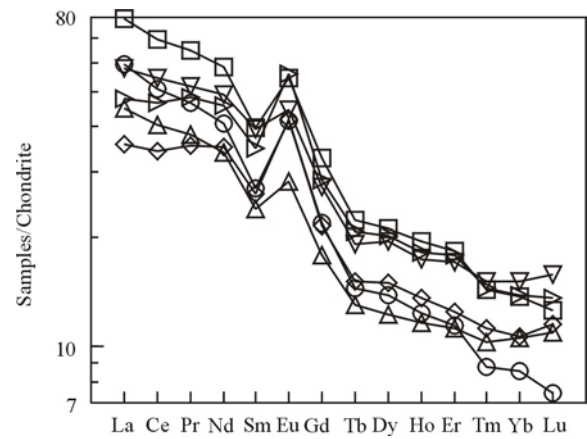


Fig. 5. Chondrite-normalized REE pattern for the Weiya gabbro. Chondrite-normalized values are from Boynton (1984).

Table 2 Sr-Nd-O isotopic data of the Weiya gabbro

Sample	x-39	x-45	x-47	x-50	x-51
Rb (ppm)	45.16	39.05	9.015	11.89	40.17
Sr (ppm)	601.2	708.1	209.8	181.4	239.6
$^{87}\text{Rb}/^{86}\text{Sr}$	0.2142	0.1531	0.1219	0.2028	0.4874
$^{87}\text{Sr}/^{86}\text{Sr}$	0.707456±8	0.707230±5	0.707205±9	0.707314±11	0.709317±8
$(^{87}\text{Sr}/^{86}\text{Sr})_i$	0.706725	0.706707	0.706789	0.706622	0.707653
average $(^{87}\text{Sr}/^{86}\text{Sr})_i$			0.7069		
Sm (ppm)	5.281	7.632	4.717	4.986	6.804
Nd (ppm)	23.98	34.73	19.85	20.33	28.02
$^{147}\text{Sm}/^{144}\text{Nd}$ ($\pm 0.5\%$)	0.1306	0.1329	0.1368	0.1446	0.1497
$^{143}\text{Nd}/^{144}\text{Nd}$	0.512561±8	0.512577±6	0.512581±9	0.512592±10	0.512603±7
$(^{143}\text{Nd}/^{144}\text{Nd})_i$	0.512356	0.512368	0.512366	0.512365	0.512368
average $(^{143}\text{Nd}/^{144}\text{Nd})_i$			0.512365		
$\varepsilon_{\text{Nd}}(t)$	0.52	0.76	0.72	0.70	0.76
$\delta^{18}\text{O}$ (‰) _{SMOW}		7.01	6.08	8.04	5.67

indicating that the magma for the Weiya gabbro underwent continental contamination, or that its source was metasomatized by subduction-related fluids (James, 1981).

5 Discussion

5.1 Crustal contamination or source contamination?

It has been documented that Th/Ta ratio in basaltic magmas, derived either from mantle lithosphere or from asthenosphere, is independent of fractional crystallization of olivine, clinopyroxene and feldspar (Aldanmaz et al., 2000). Thus, the Th/Ta ratio would fall within or close to that of the diagonal mantle array defined by constant Th/Ta ratio (Fig. 6). Source metasomatism by subduction-related fluids, however, results in enrichment of Th with respect to Ta, as subduction-related fluids are generally enriched in Th relative to Ta (Aldanmaz et al., 2000). Consequently, magma derived from such a metasomatized source would result in enrichment in Th relative to Ta, and hence show higher Th/Ta ratio than the diagonal mantle array (Fig. 6). Also, mantle-derived magma affected by crustal contamination may increase in Th/Ta ratio because

of the higher crustal abundances in Th with respect to Ta, with the exception of the granulite facies crust, which has low Th contents (Aldanmaz et al., 2000).

As shown in Fig. 6, all samples of the Weiya gabbro exhibit higher Th/Ta ratios relative to the mantle array. This could be interpreted as the result of either source metasomatism by subduction-related fluids, or contamination by continental crust, or even both. However, crustal contamination could be precluded by consideration of two factors below.

Firstly, ratios of Ti/Zr and Ti/Y of mantle-derived magmas affected by crustal contamination are lower than those of parent magmas due to lower ratios of Ti/Zr and Ti/Y in crustal rocks (Ti/Zr < 30, Ti/Y < 200; see Wedepohl, 1995). Figure 7 shows that Ti/Zr goes in an opposite trend to Ti/Y as CaO and MgO decrease gradually. No synchronously lowering trends between Ti/Zr and Ti/Y have been found, indicating that Ti/Zr and Ti/Y are mainly controlled by fractional crystallization instead of crustal contamination. Moreover, crustal contamination is clearly insignificant for the Weiya gabbro based on high Ti/Zr ratios ranging from 52.79 to 151.58 with an average of 86.01 and Ti/Y ratios varying from 240.56 to 615.23 with an average of 467.32.

Secondly, as indicated by James (1981), if the mantle source (either mantle lithosphere or asthenosphere) suffered from metasomatism (*source contamination*) by subduction-related fluids, then trace element and Sr isotope compositions of the partial melts would be dominated by slab-derived compositions, whereas O isotope and major elements of the melt would be dominated by materials from the overlying mantle wedge. Consequently, a concave curve would appear in $\delta^{18}\text{O}$ vs. $^{87}\text{Sr}/^{86}\text{Sr}$ and $\delta^{18}\text{O}$ vs. $^{143}\text{Nd}/^{144}\text{Nd}$ diagrams. In contrast,

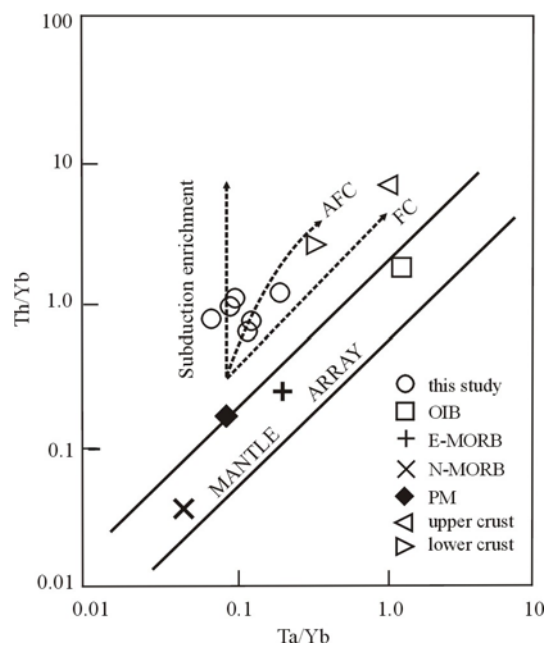


Fig. 6. Th/Yb against Ta/Yb log-log diagram for the Weiya gabbro (after Aldanmaz et al., 2000). PM: primitive mantle; Data of OIB, N-MORB, E-MORB and PM are from Sun and McDonough (1989); Data of upper crust and lower crust are from Wedepohl (1995).

mixing curves from **crustal contamination** in the $\delta^{18}\text{O}$ vs. $^{87}\text{Sr}/^{86}\text{Sr}$ and $\delta^{18}\text{O}$ vs. $^{143}\text{Nd}/^{144}\text{Nd}$ would typically be convex. It follows that concave curves for the Weiya gabbro in the $\delta^{18}\text{O}$ vs. $^{87}\text{Sr}/^{86}\text{Sr}$ and $\delta^{18}\text{O}$ vs. $^{143}\text{Nd}/^{144}\text{Nd}$ diagrams (Fig. 8) should be indicative of source contamination rather than crustal contamination.

5.2 Source of slab-derived fluids

Elemental and isotope geochemistry indicate that the source region for the Weiya gabbro was metasomatized by slab-derived fluids, and that assimilation of the mantle-derived magma by continental crust during ascent is clearly insignificant. The key problem is whether the source metasomatism is induced by subducted continental or oceanic crust. Research of trace element geochemistry would help to discriminate. It is a common practice to adopt a very simplified lithological section through the oceanic lithosphere that includes an upper layer of hemipelagic sediments and altered oceanic crust (~95 wt%), and a lower layer of depleted peridotite (Poli and Schmidt, 2002). Despite that hemipelagic sediments are enriched in Ba, Rb, K and Pb (Patino et al., 2000), Rb and Pb are prone to enter hydrothermal fluids and hence would be preferentially removed during seawater alteration. In contrast, U can be moderately enriched, and Th and REE remain unmodified during alteration (Chauvel et al., 1995). Therefore, the resultant mantle-derived magma from partial melting of overlying mantle wedge which was metasomatized by oceanic subduction-related fluids would be characterized by enrichment of Ba, K and U and

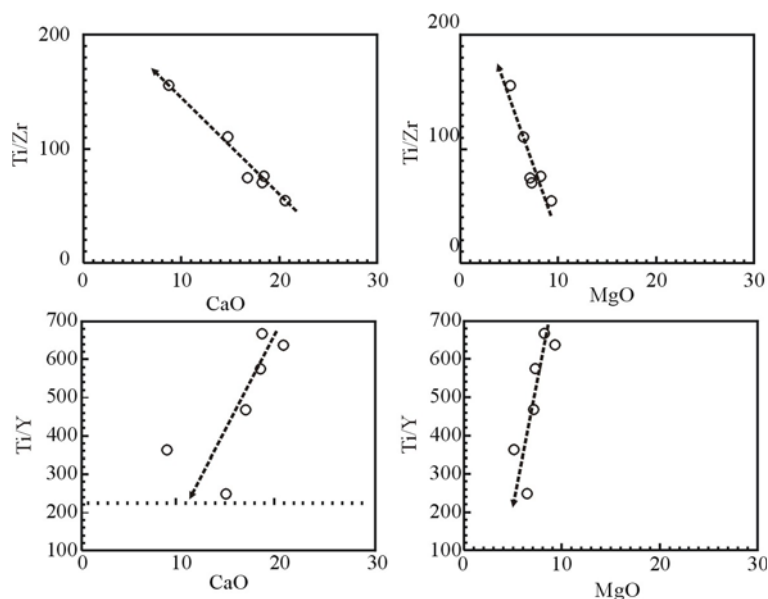


Fig. 7. Plots of Ti/Zr vs. CaO (wt%), Ti/Zr vs. MgO (wt%), Ti/Y vs. CaO (wt%) and Ti/Y vs. MgO (wt%) for the Weiya gabbro.

depletion of Rb and Pb, as well as high ratios of U/Pb and Ce/Pb, and low ratios of Th/U (Walker et al., 2001).

In so far as the Weiya gabbro is concerned, the rock appears to be enriched both in Ba, K and U and in Rb and Pb, with virtually low ratios of Ce/Pb (5.74–10.16, Table 1), which are substantially lower than those of altered oceanic crust (400–500, Klein and Karsten, 1995), indicating that source metasomatism is unlikely related to oceanic subduction. On the other hand, significantly negative Nb anomaly (Fig. 4) of the Weiya gabbro is the most characteristic of subduction zone volcanic rocks or typical continental rocks. As mentioned above, however, since oceanic subduction and during-magma-ascent continental contamination are not considered plausible, the “continental” signature of the Weiya gabbro should have been printed on its source region. Moreover, the ratios (Table 1) of La/Nb (averaging 6.67) and Ba/Nb (averaging 399.74) of the Weiya gabbro are substantially higher than those of MORB and OIB, which have La/Nb ratios ranging from 0.5 to 2.5 and much smaller Ba/Nb ratios varying from 20 to 1 (Jahn et al., 2004). High ratios of La/Nb and Ba/Nb are commonly ascribed to significant involvement of continental materials in the mantle source in the absence of both during-magma-ascent continental contamination and oceanic subduction (Jahn et al., 2004). Therefore, metasomatism by fluids or melts from subducted continental crust is likely to have occurred to the overlying source region in mantle wedge prior to the generation of the magma for the Weiya gabbro.

Compared to the mafic-ultramafic intrusions in the Dabie Mountains, which have been interpreted to be derived from metasomatized mantle modified by fluids released from subducted continental crust (Li et al.,

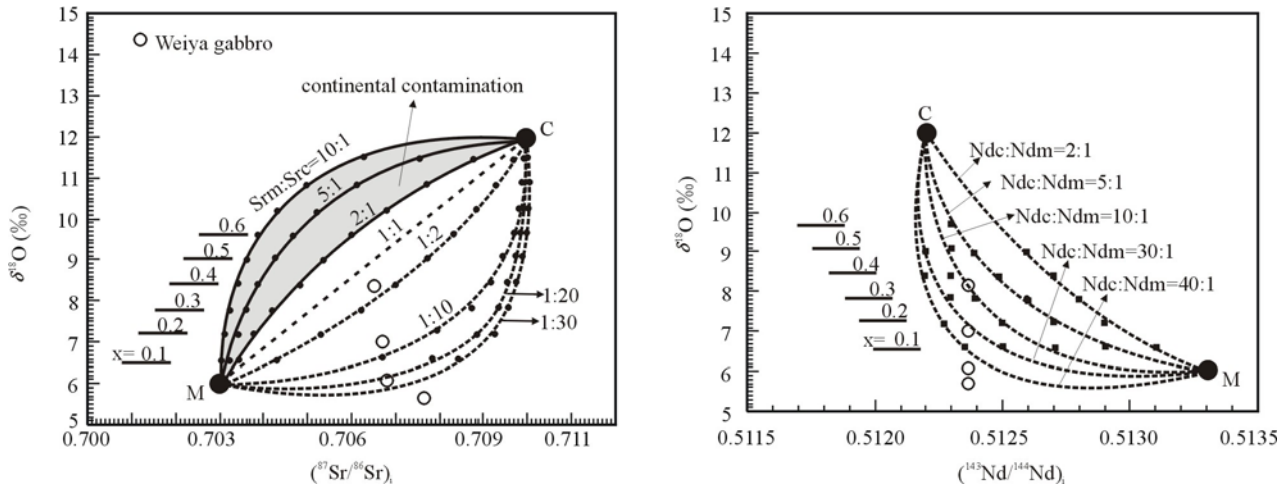


Fig. 8. Theoretical mantle source M and contaminant C (subducted slab or continental crust) mixing curves of $\delta^{18}\text{O}$ vs. $(^{87}\text{Sr}/^{86}\text{Sr})_i$ and $\delta^{18}\text{O}$ vs. $(^{143}\text{Nd}/^{144}\text{Nd})_i$ (after James, 1981).

End member M: $\delta^{18}\text{O}=6$ (‰)_{SMOW}, $(^{87}\text{Sr}/^{86}\text{Sr})_i=0.703$, $(^{143}\text{Nd}/^{144}\text{Nd})_i=0.5133$; End member C: $\delta^{18}\text{O}=12$ (‰)_{SMOW}, $(^{87}\text{Sr}/^{86}\text{Sr})_i=0.710$, $(^{143}\text{Nd}/^{144}\text{Nd})_i=0.5123$ (after James, 1981). In the plot of $\delta^{18}\text{O}$ vs. $(^{87}\text{Sr}/^{86}\text{Sr})_i$, Sr_M and Sr_C are indicative of Sr contents of mantle end member (M) and subducted slab or continent crust (C), respectively. When the ratio of Sr_M to Sr_C (Sr_M/Sr_C) is greater than 2:1, it implies continental contamination during mantle-derived magma ascent and emplacement. In contrast, when the ratio of Sr_M to Sr_C (Sr_M/Sr_C) is less than 1:2, it indicates source contamination. In the plot of $\delta^{18}\text{O}$ vs. $(^{143}\text{Nd}/^{144}\text{Nd})_i$, Nd_M and Nd_C are indicative of Nd contents of mantle end member (M) and subducted slab or continent crust (C), respectively. Ratio shown with each curve denotes proportion of Sr (or Nd) content of M (Sr_M or Nd_M) to Sr (or Nd) content of C (Sr_C or Nd_C), x denotes weight proportion of component C to component M.

It is indicated from Fig. 8 that the source region of the Weiya gabbro was contaminated by slab-derived fluids (source contamination), with limited continental contamination during magma ascent and emplacement.

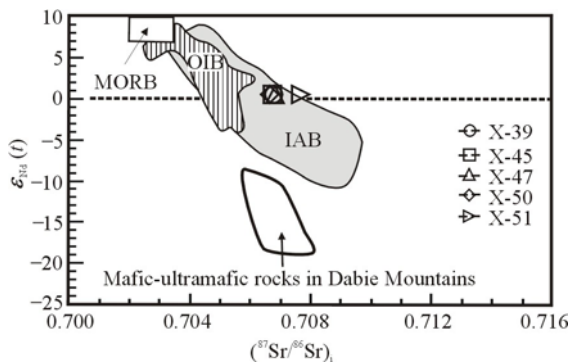


Fig. 9. Plot of $\epsilon_{\text{Nd}}(t)$ vs. $(^{87}\text{Sr}/^{86}\text{Sr})_i$ for the Weiya gabbro (after Li et al., 1998b).

MORB – Middle ocean ridge basalts (Sun and McDonough, 1989); OIB – oceanic island basalts (Zindler and Hart, 1986); IAB – island arc basalts (Davidson, 1983); mafic-ultramafic rocks in Dabie Mountains (Li et al., 1998b).

1998b), the Weiya gabbro has initial Sr values similar to, but $\epsilon_{\text{Nd}}(t)$ values (>0) higher than the mafic-ultramafic intrusions in the Dabie Mountains (Fig. 9). Therefore, petrogenesis of the Weiya gabbro is distinguishable from that of mafic-ultramafic rocks in the Dabie Mountains, which were derived from mantle modified by fluids released from subducted ancient craton (Yangtze Craton) with characteristic of significantly negative $\epsilon_{\text{Nd}}(t)$ values (Li et al., 1998b). In contrast, the Weiya gabbro has initial $^{87}\text{Sr}/^{86}\text{Sr}$ and $\epsilon_{\text{Nd}}(t)$ values falling within the ranges of island arc basalts (IAB, Fig. 9), but distinctly different from both mafic-ultramafic intrusions in the Dabie Mountains and MORB or OIB (Fig. 9). Therefore, the Weiya gabbro is most likely derived from metasomatized mantle which was modified by fluids released from

subducted young continental crust instead of ancient craton basement in intraplate settings during the Indosinian. It remains to be investigated, however, whether the subducted young continental crust is the Qoltag island arc (Fig. 1) or some other young terrane north to the Middle Tianshan Mountains, and where the location of subduction zone is.

6 Conclusion: Tectonic Implications

From the foregoing sections, we suggest that the source region of the Weiya gabbro was metasomatized by fluids released from young subducted continental crust with limited crustal contamination during the magma ascent and emplacement. It has been indicated that the Weiya gabbro was formed in the early Triassic (Zhang et al., 2005) when the Middle Tianshan areas were situated in an intraplate setting (Gu et al., 2006). Numerous Indosinian granites (Xu et al., 2001; Jiang et al., 2003; Li et al., 2005) have been reported from the Middle Tianshan Mountains and adjacent areas such as those in the Beishan Mountains and eastern Kunlun Mountains. This indicates that Indosinian tectono-thermal events were active in the Middle Tianshan Mountains and adjacent areas. As a consequence, we would link the Indosinian tectono-thermal events in the Middle Tianshan Mountains and adjacent areas genetically to the northward subduction of the Paleo-Tethyan oceanic plate during the Late Permian to Triassic (Guo et al., 1998). It is just the northward subduction of this plate that induced intense southward subduction of some young terrane north to the Middle

Tianshan Mountains. Such an inference is consistent with the conclusion of Zhang et al. (2006), who, based on research of the quartz syenite within the Weiya complex, proposed that crustal thickening in the Tianshan area during the Indosinian was likely to have been caused by intra-continental (A-type) subduction of the Tianshan area, which, in its turn, was induced by northward subduction of the Paleo-Tethyan oceanic crust from the Late Permian to Triassic. This is consistent with the conclusion of Xiao et al. (1992) and Li and Xiao (1999), who, based on tectonic research of the eastern Tianshan Mountains, proposed that intense Triassic (Indosinian) compression of this area was induced by the northward subduction of the Paleo-Tethyan ocean plate.

In summary, we emphasize that a new tectonic system caused the Indosinian tectono-thermal events in the study area and that tectonic conversion from the Paleo-Asian to the Paleo-Tethys regime occurred during the latest Permian or Earliest Triassic. From such a point of view, further research on Indosinian magmatism would be of particular importance to clarify geological evolution of the Tianshan orogenic belt and adjacent areas in the Triassic Period.

Acknowledgements

Prof. Zhou Jincheng from the Department of Earth Sciences of Nanjing University is acknowledged for his comments on the original manuscript. Special thanks should be given to anonymous reviewers, whose constructive comments and suggestions have greatly contributed to the improvement of this manuscript. This study was jointly supported by National Natural Science Foundation of China (Nos. 40672040, 40472042 and 40603008), National Basic Research Program of China (2001CB409802), and China Postdoctoral Science Foundation (No. 2005038237) and Laboratory for Radiogenic Isotope Geochemistry, Institute of Geology and Geophysics, Chinese Academy of Sciences.

Manuscript received Dec. 5, 2005

accepted Aug. 8, 2006

edited by Xie Guanglian and Zhang Xinyuan

References

- Aldanmaz, E., Pearce, J.A., and Thirlwall, M.F., 2000. Petrogenetic evolution of late Cenozoic post-collision volcanism in western Anatolia, Turkey. *Journal of Volcanology and Geothermal Research*, 102: 67–95.
- Boynton, W.V., 1984. Geochemistry of the rare earth elements: meteorite studies. In: Henderson P. (ed.), *Rare Earth Element Geochemistry*. Amsterdam: Elsevier Science Publishers, 63–114.
- Chauvel, C., Goldstein, S.L., and Hofmann, A.W., 1995. Hydration and dehydration of oceanic crust controls Pb evolution in the mantle. *Chem. Geol.*, 126: 65–75.
- Davidson, J.P., 1983. Lesser Antilles isotopic evidence of the role of subducted sediment in island arc magma genesis. *Nature*, 306:253–256
- Frey, F.A., Roden, M.F., and Zindler, A., 1980. Constraints on mantle source compositions imposed by phosphorus and the rare-earth elements. *Contrib. Mineral. Petrol.*, 75:165–173.
- Gao Jianfeng, Lu Jianjun and Lai Mingyuan, 2003. Analysis of trace elements in rock samples using HR-ICPMS. *J. Nanjing Univ. (Natural Sci.)*, 39(6): 844–850 (in Chinese with English abstract).
- Gu Lianxing, Yang Hao, Tao Xiancong, Yan Zhenfu, Li Huimin, Wang Jinzhu and Liu Yandong, 1990. Rb-Sr geochronology and the tectonic evolution of the east section of the Middle Tianshan Mountains. *Journal of Guilin College of Geology*, 10: 49–55 (in Chinese with English abstract).
- Gu Lianxing, Yang Hao, Yan Zhengfu and Liao Jingjuan, 1996. Geology and genesis of peraluminous granites in East Tianshan Upper Paleozoic island arc belt. *Chinese J. Geochem.*, 15(1): 33–43.
- Gu Lianxing, Hu Shouxi, Chu Qiang and Xiang Xinjian, 1999. Pre-collision granites and post-collision intrusive assemblage of the Kelameili-Harlik orogenic belt. *Acta Geologica Sinica* (English edition), 73(3): 316–329.
- Gu Lianxing, Hu Shouxi, Yu Chunshui, Zhao Ming, Wu Changzhi and Li Hongyu, 2001. Intrusive activities during compression-extension tectonic conversion in the Bogda intra-continental orogen. *Acta Petrologica Sinica*, 17(2): 187–198 (in Chinese with English abstract).
- Gu Lianxing, Gou Xiaoqin, Zhang Zunzhong, Wu Changzhi, Liao Jinjuan, Yang Hao, Yin Lin and Min Maozhong, 2003. Geochemistry and petrogenesis of a multi-zoned high Rb and F granite in eastern Tianshan. *Acta Petrologica Sinica*, 19(4): 585–600 (in Chinese with English abstract).
- Gu Lianxing, Zhang Zunzhong, Wu Changzhi, Wang Yinxi, Tang Junhua, Wang Chuansheng, Xi Aihua and Zheng Yuanchuan, 2006. Some problems on granites and vertical growth of the continental crust in the eastern Tianshan Mountains, NW China. *Acta Petrologica Sinica*, 22(5): 1103–1120 (in Chinese with English abstract).
- Guo Zhaojie and Zhang Zhicheng, 1993. On the Early Paleozoic island arc belt of Mid-Tianshan. *Journal of Hebei College of Geology*, 16(2): 132–139 (in Chinese with English abstract).
- Guo Zhengfu, Deng Jinfu, Xu Zhiqin, Mo Xuanxue and Luo Zhaohua, 1998. Late Paleozoic-Mesozoic intra-continental orogenic process and intermediate acidic igneous rocks from the eastern Kunlun Mountains of northwestern China. *Geoscience*, 12(3):344–352 (in Chinese with English abstract).
- Han Baofu, He Guoqi and Wang Shiguang, 1999. Post-collisional mantle-derived magmatism, underplating and implications for basement of the Junggar Basin. *Sci. China (D)*, 42(2): 113–119.
- Han, B.F., Wang, S.G., Jahn B.M., Hong, D.W., Kagami, H., and Sun, Y.L., 1997. Depleted-mantle source for the Ulungur River A-type granites from North Xinjiang, China: geochemistry and Nd-Sr isotopic evidence, and implications for Phanerozoic crustal growth. *Chem. Geol.*, 138: 135–159.
- Hong, D.W., Zhang, J.S., Wang, T., Wang, S.G., and Xie X.L., 2004. Continental crustal growth and the supercontinental cycle: evidence from the Central Asian Orogenic Belt. *J. Asian Earth Sci.*, 23: 799–813.
- Hu Aiqin, Wang Zhonggang and Tu Guangchi, 1997. *Geological Evolution, Petrogenesis and Metallogeny of North Xinjiang*. Beijing: Science Press, 246 (in Chinese).
- Hu, A.Q., Jahn, B.M., Zhang, G.X., Chen, Y.B., and Zhang, Q.F., 2000. Crustal evolution and phanerozoic crustal growth in northern Xinjiang: Nd isotopic evidence. Part I. Isotopic characterization of basement rocks. *Tectonophysics*, 328: 15–51.

- Hu Shouxi, Guo Jichun and Gu Lianxing, 1990. Geology of the Caledonian orogenic belt and its importance to the framework of East Tianshan (E 85°–95°). *Geoscience of Xinjiang*, 1: 32–45 (in Chinese).
- Jahn, B.M., Wu, F.Y., and Chen, B., 2000. Granitoids of the Central Asian orogenic belt and continental growth in the Phanerozoic. *Trans. R. Soc. Edinburgh: Earth Sci.*, 91: 181–193.
- Jahn, B.M., Wu, F.Y., Lo, C.H., and Tsai, C.H., 2004. Crust-mantle interaction induced by deep subduction of the continental crust: geochemical and Sr-Nd isotopic evidence from post-collisional mafic-ultramafic intrusions of the northern Dabie complex, central China. *Chem. Geol.*, 157: 119–146.
- James, D.E., 1981. The combined use of oxygen and radiogenic isotopes as indicators of crustal contamination. *Ann. Rev. Earth Sci.*, 9: 311–344.
- Jiang Sihong, Nie Fengjun, Chen Wen, Liu Yan, Bai Daming, Liu Xinyu and Zhang Sihong, 2003. The determination of the emplacement age of granite in Mingshui, Beishan area, and its implication. *Acta Petrologica et Mineralogica*, 22(2): 107–111 (in Chinese with English abstract).
- Klein, E.M., and Karsten, J.L., 1995. Ocean-ridge basalts with convergent-margin geochemical affinities from the Chile Ridge. *Nature*, 374: 52–57.
- Kyser, T.K., 1990. Stable isotopes in the continental lithospheric mantle. In: Menzies, M.A. (ed.), *Continental Mantle*. Oxford: Clarendon Press, 127–156.
- Langmuir, C.H., Bender, J.F., and Bence, A.E., 1977. Petrogenesis of basalts from the famous area: mid-Atlantic ridge. *Earth Planet. Sci. Lett.*, 36: 133–156.
- Li Shuguang, Nie Yonghong, Liu Deliang and Zheng Shuanggen, 1998a. Interaction between subducted continental crust and the mantle I: Major and trace element geochemistry of the syncollisional mafic-ultramafic intrusions in the Dabie Mountains. *Sci. China (D)*, 41(5): 545–552.
- Li Huaqin, Chen Fuwen, Lu Yuanfa, Yang Hongmei, Guo Jing and Mei Yuping, 2005. New chronological evidence for Indosinian diagenetic mineralization in eastern Xinjiang, NW China. *Acta Geologica Sinica (English edition)*, 79(2): 264–275.
- Li Jinyi and Xiao Xuchang, 1999. Brief reviews on some issues of framework and tectonic evolution of Xinjiang crust, NW China. *Scientia Geologica Sinica*, 34(4): 405–419 (in Chinese with English abstract).
- Li, J.Y., Xiao, W.J., Wang, K.Z., Sun, G.H., and Gao, L.M., 2003. Neoproterozoic-Paleozoic tectonostratigraphy, magmatic activities and tectonic evolution of Eastern Xinjiang, NW China. In: Mao Jinwen, Goldfarb, R.J., Seltmann, R., Wang Denghong, Xiao Wenjiao and Hart, C. (eds), *Tectonic Evolution and Metallogeny of the Chinese Altay and Tianshan. Proceedings Volume of the International Symposium of the IGCP-473 Project in Urumqi and Guidebook of the Field Excursion in Xinjiang, China*. August 9–21, IAGOD Guidebook Series 10: CERCAMS/NHM London, 31–74.
- Li Shuguang, Nie Yonghong, Hart, S.R., and Zhang Zongqing, 1998b. Interaction between subducted continental crust and the mantle II. Sr and Nd isotopic geochemistry of the syncollisional mafic-ultramafic intrusions in Dabie Mountains. *Sci. China (D)*, 41(6): 632–638.
- Patino, L.C., Carr, M.J., Feigenson, M.D., 2000. Local and regional variations in Central American arc lavas controlled by variations in subducted sediment input. *Contrib. Mineral. Petrol.*, 138: 265–283.
- Poli, S., and Schmidt, M.W., 2002. Petrology of subducted slabs. *Ann. Rev. Earth Planet. Sci.*, 30: 207–235.
- Shu Liangshu, Charvet, J., Guo Lingzhi, Lu Huaifu and Laurent-Charvet, S., 1999. A large-scale Paleozoic dextral ductile strike-slip zone: the Aqqikkudug-Weiya zone along the Northern Margin of the Central Tianshan belt, Xinjiang, NW China. *Acta Geologica Sinica (English edition)*, 73(2): 148–162.
- Smith, J.V., 1981. Halogen and phosphorus storage in the earth. *Nature*, 189:762–765.
- Sun, S.S., and McDonough, W.F., 1989. Chemical and isotopic systematics of oceanic basalts: implications for mantle composition and processes. In: Saunderson, A.D., Norry, M.J. (ed.), *Magmatism in the Ocean Basins*, Geol. Soc. Spec. Pub., 42: 313–345.
- Xia Linqi, Xia Zuchun, Xu Xueyi, Li Xiangmin, Ma Zhongpig and Wang Lishe, 2005. Relationships between basic and silicic magmatism in continental rift settings: A petrogeochemical study of Carboniferous post-collisional silicic volcanics in Tianshan, NW China. *Acta Geologica Sinica (English edition)*, 79(5): 633–653.
- Xiao Xuchang, Tang Yaoqing, Feng Yimin, Zhu Baoqing, Li Jinyi and Zhao Min, 1992. *Tectonic Evolution of Northern Xinjiang and Its Adjacent Regions*. Beijing: Geological Publishing House, 169 (in Chinese with English abstract).
- Xu Zhiqin, Yang Jinsui and Jiang Mei, 2001. Collision-orogeny of the Northern Qinghai-Tibet plateau and its deep dynamics. *Acta Geoscientia Sinica*, 22(1): 5–10 (in Chinese with English abstract).
- Walker, J.A., Patino, L.C., and Carr, M.J., 2001. Slab control over HSE depletions in central Nicaragua. *Earth Planet. Sci. Lett.*, 192: 533–543.
- Wang Yinxi, Yang Jiedong, Tao Xiancong and Li Huimin, 1988. A study of the Sm-Nd method for fossil mineral and rock and its applications. *J. Nanjing Univ. (Natural Sci.)*, 24(2): 297–308 (in Chinese with English abstract).
- Wedepohl, K.H., 1995. The composition of the continental crust. *Geochim. Cosmochim. Acta*, 59: 1217–1232.
- Wu Changzhi, Zhang Zunzhong, Zaw, K., Della-Pasque, F., Tang Junhua, Zheng Yuanchuan, Wang Chuansheng and San Jinzhu, 2006. Chronology, geochemistry and tectonic significances of the Hongyuntan granitoids in the Qoltag area, Eastern Tianshan. *Acta Petrologica Sinica*, 22(5): 1121–1134 (in Chinese with English abstract).
- Zhang Zunzhong, Gu Lianxing, Wu Changzhi, Li Weiqiang, Xi Aihua and Wang Shuo, 2005. Zircon SHRIMP dating for the Weiya pluton, eastern Tianshan: its geological implications. *Acta Geologica Sinica (English edition)*, 79(4): 481–490.
- Zhang Zunzhong, Gu Lianxing, Wu Changzhi, Zhai Jianping, Xi Aihua, Li Weiqiang, and Tang Junhua, 2006. The quartz syenite within the Weiya complex from the eastern Tianshan: petrography, geochemistry and petrogenesis. *Acta Petrologica Sinica*, 22(5): 1135–1149 (in Chinese with English abstract).
- Zhao Zhenhua, Xiong Xiaolin, Wang Qiang, Bai Zhenghua, Xu Jifeng and Qiao Yulou, 2004. Association of late Paleozoic adakitic rocks and shoshonitic volcanic rocks in the western Tianshan, China. *Acta Geologica Sinica (English edition)*, 78 (1): 68–72.
- Zhou, M.F., Leshner, C.M., Yang, Z.X., Li, J.W., and Sun, M., 2004. Geochemistry and petrogenesis of 270 Ma Ni-Cu-(PGE) sulfide-bearing mafic intrusions in the Huangshan district, Eastern Xinjiang, Northwest China: implications for the tectonic evolution of the Central Asian Orogenic Belt. *Chem. Geol.*, 209: 233–257.
- Zindler, A., and Hart, S., 1986. Chemical geodynamics. *Ann. Rev. Earth Planet. Sci.*, 14: 493–571.